Sc and Er co-doped AlN surface acoustic wave devices

Shiping Mao[1,2], Zixiong Ru[1,2], Chengtao Yang[1,2], Jian Zhou[3,*], Jianhui Wu[3], Yongqing Fu[4]*

[1.] State Key Laboratory of Electronic Thin Films and Integrated Devices, University of Electronic Science and Technology of China, Chengdu 611731, People's Republic of China

[2.] Yangtze Delta Region Institute (Huzhou) ， University of Electronic Science and Technology of China, Huzhou 313001, P. R. China

[3.] College of Mechanical and Vehicle Engineering, Hunan University, Changsha 410082, People's Republic of China

[4.] Faculty of Engineering and Environment, Northumbria University, Newcastle upon Tyne, NE1 8ST, United Kingdom

*E-mail: 592967553@qq.com, jianzhou@hnu.edu.cn.

All authors:

1. Shiping Mao; Email: 13883674379@139.com;
2. Zixiong Ru; Email: eggplant.Ru@outlook.com;
3. Chengtao Yang; Email: 592967553@qq.com;
4. Jian Zhou; Email: jianzhou@hnu.edu.cn;
5. Jianhui Wu; Email: 2092302748@qq.com;
6. Yongqing Fu； Email: Richard.Fu@northumbria.ac.uk;

ABSTRACT: Co-doping AlN film with various elements of rare earth or transition metals has been considered as a good method to significantly improve its piezoelectric responses of surface acoustic wave (SAW) devices. In this paper, we investigated the influences of different Er/Sc atomic percentage ratio on the piezoelectric and acoustic wave properties of the Er and Sc co-doped AlN films prepared by RF magnetron sputtering. Results show that *c/a*-axis ratio of the AlN films decreases after doped with Sc, whereas those of the AlN films co-doped with Er and Sc increase as the Er/Sc ratio increases. The reasons can be explained from the competitions of Sc and Er elements for occupying the Al atoms sites, and the larger ion radius of the Er compared that of Sc, which causes significant increase of *c/a*. Resonant frequency and Rayleigh wave velocity of the SAW resonators fabricated using these co-doped AlN films decrease as the Er/Sc ratio increases. Electromechanical coupling coefficient (k^2_{eff}) of the SAW devices increases after the AlN film is single doped with either Sc or Er element, but decreases after co-doping with both Er and Sc.

KEYWORDS: Er-Sc co-doped AlN film, effective electromechanical coupling coefficient, *c/a*-axis ratio

1. Introduction

Aluminum nitride (AlN) has good properties such as high sound velocity, high breakdown voltage [1], good thermal conductivity [2], high hardness [3], and excellent chemical and thermal stabilities. It is also compatible with the CMOS technology, and has been regarded as one of the best materials for high-frequency surface acoustic wave (SAW) resonators [4] and RF communication systems [5]. However, the piezoelectric coefficient (d_{33}) of the pure AlN film is about 5.5 pc/N, the electromechanical coupling coefficient (k^2_{eff}) is 6%~7% and that of corresponding SAW device is 2%, which are relatively low and limit the fractional bandwidth of the SAW RF filters [6, 7]. Recent studies have found that doping the AlN with rare earth metals or transition metals can significantly improve its piezoelectric response and k^2_{eff} [8]. The k^2_{eff} of $Sc_xAl_{1-x}N$ increases from 7% to 10% with the increase of the Sc contents. [9] Based on the results of Mg-Nb doping AlN films and Sc doped III-nitrides reported in Ref. [10, 11], when the *c/a* axis ratio decreases, the stiffness coefficient C_f decreases, and the phase change barrier of non-polar to polar structures decreases. Thus, the piezoelectric response get improved. Both experimental results and first-principles calculations showed that these doping elements cause the softening of AlN crystal structures and the decrease of energy barrier from *w*-AlN to *h*-AlN crystalline structures, thus significantly improving piezoelectric responses of wurtzite alloys AlN doped with Sc, Er, Y and Mg/Zr elements [12, 13]. Among the various doping elements investigated, Sc has showed the best improvement in d_{33} value for the doped AlN film [6, 12]. With an increase in the doping concentration of Sc, the piezoelectricity is enhanced monotonically up to 43% of scandium concentration, and the obtained piezoelectric coefficient d_{33} is five times larger than that of pure AlN [13]. However, Sc is one rare earth element and thus doping with large amounts of Sc elements will significantly increase the price of the materials. Recent studies also show that minor addition of Er can increase the d_{33} values, *c*-axis preferred orientation and piezoelectric responses of AlN films [14, 15].

However, currently Er-doped AlN film based SAW devices have never been reported, and there are few studies about the Sc and Er co-doped AlN films. It is critical to investigate and clarify what the co-doping mechanism is after the AlN film is doped with both Er and Sc, and what the changes are for electrical/structural characteristics and piezoelectric response of the co-doped films.

In this paper, we deposited Er and Sc co-doped AlN films with different ratios of Er and Sc atomic contents using reactive magnetron sputtering. Electrical and structural characteristics of the prepared films have been systematically investigated. SAW devices based on these films have been fabricated and characterized, and the mechanisms and effects of doping of these elements for the changes of piezoelectric and acoustic wave properties were systematically studied.

2. Experimental

The *c*-axis oriented $Er_xSc_yAl_{1-x-y}N$ films were deposited on (0001) sapphire substrates using an RF magnetron sputter. Prior to the deposition, the sapphire substrate was cleaned in the ultrasonic baths with acetone, absolute ethyl alcohol and deionized water in sequence. The base vacuum of the sputter chamber was ~4×10^{-4} Pa. Elemental contents, crystalline structures, surface topography, and film thickness of the deposited films were characterized using energy dispersive X-ray spectroscopy (EDX) glancing incident X-ray diffractometer (GIXRD, PANayltical Empyrean), atomic force microscope (AFM, SPA-300HV) and ellipsometer (JA Woollam Co, Inc

RC2), respectively.

To study the SAW propagation characteristics of the $Er_xSc_yAl_{1-x-y}N$ film on the sapphire substrate, two-port SAW resonators were designed and fabricated. Figure 1 shows the IDT picture of SAW devices. Aluminum was used as the electrodes (with a thickness of 150 nm) and each SAW transducer was consisted of 80 pairs of IDT fingers, with a wavelength λ of 16 μm. The distance between the two IDT transducers was 10 λ. The aperture was 20 λ and the distance between the IDTs and the adjacent shorted reflecting gratings was designed as 1 λ to ensure the formation of a perfect standing wave at the center frequency. The transmission characteristics were measured using an Agilent E5071C network analyzer.

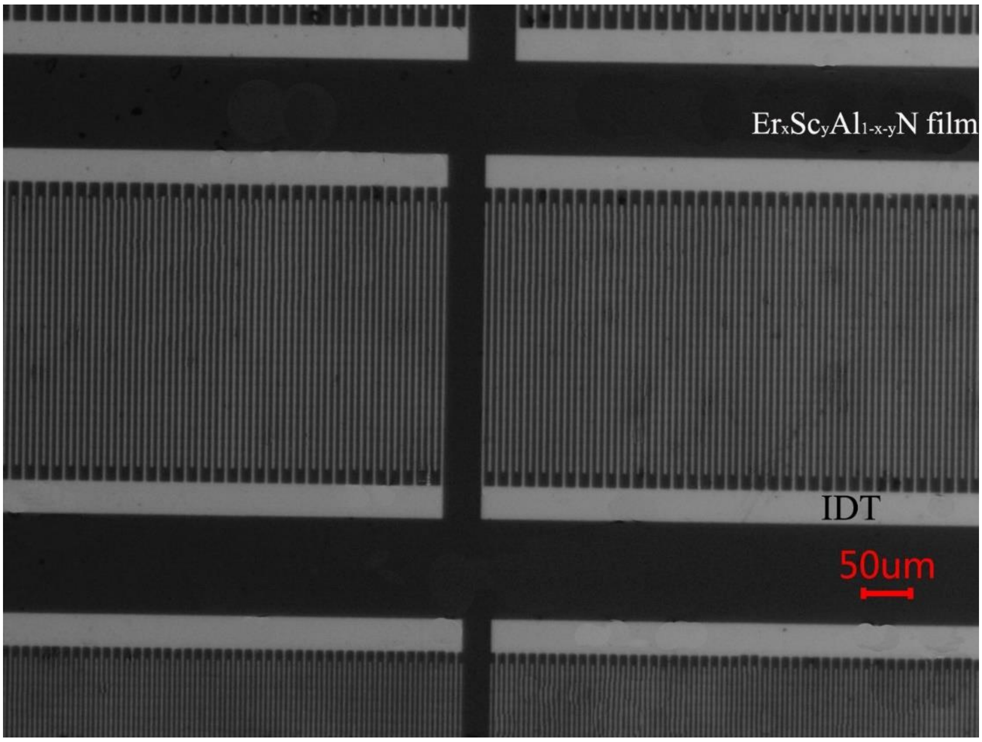

Figure.1 the picture of the SAW device

3. Results and discussion

Figure 2 shows crystalline structures of the deposited AlN piezoelectric films on the sapphire substrate with different contents of doping elements, obtained using the GIXRD. All the films exhibit (0002) preferred orientation of wurtzite AlN, with the strong XRD diffraction angle at ~36°. The diffraction angle at 42°represents the peak of sapphire substrate.

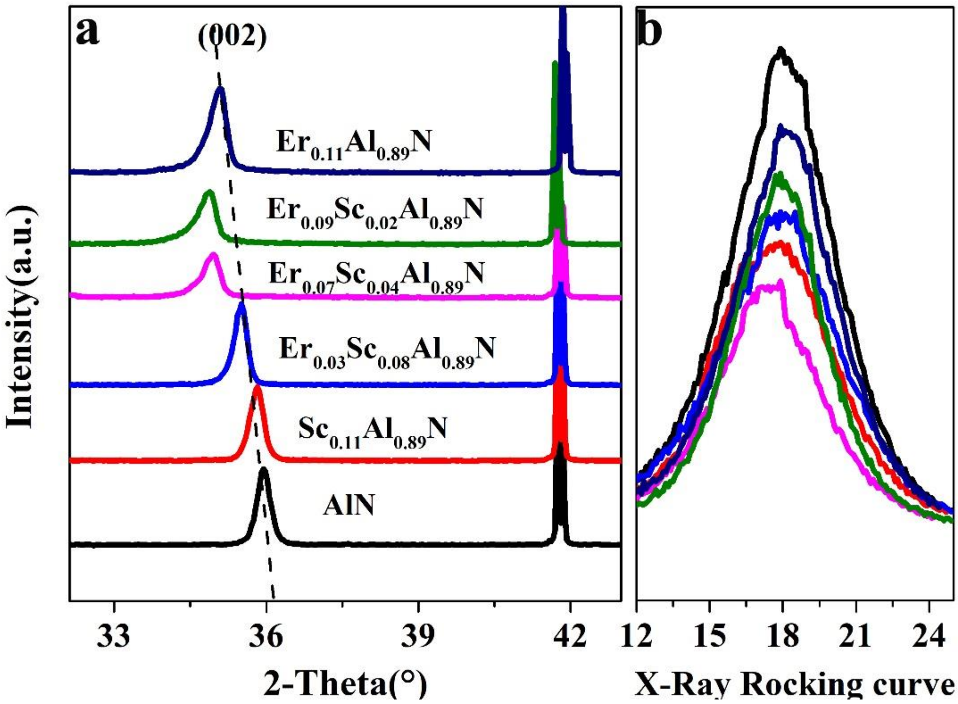

Figure 2 (a) XRD and (b) rocking curve of the Er and Sc co-doped films

With the increase of Er contents, the XRD diffraction angles of (0002) peak were found to decrease slightly (when x<0.11). This is because the incorporation of Sc and Er atoms into AlN films results in an elongation of the Al (Sc)-N and Al (Er)-N bonds. The crystal lattice of $Er_{0.11}Al_{0.89}N$ film is relatively well-ordered compared with those of $Sc_{0.09}Er_{0.02}Al_{0.89}N$ and $Sc_{0.07}Er_{0.04}Al_{0.89}N$ films, for some Sc atoms are located at the non-lattice interstitial sites and cause the lattice distortion [16]. The full width half maximum (FWHM) values of the peaks for all the films (obtained using the Rocking curves shown in Figure 1(b)) decrease from 5.67 to 4.64 as the amount of Er increases. This clearly indicates that the texture of the (0002) preferred orientation is improved when the Er doping content is increased, owing to the Er^{3+} elements are preferentially aligned with normal to *c*-axis of the AlN film during sputtering [14, 15], as illustrated in Figure 3.

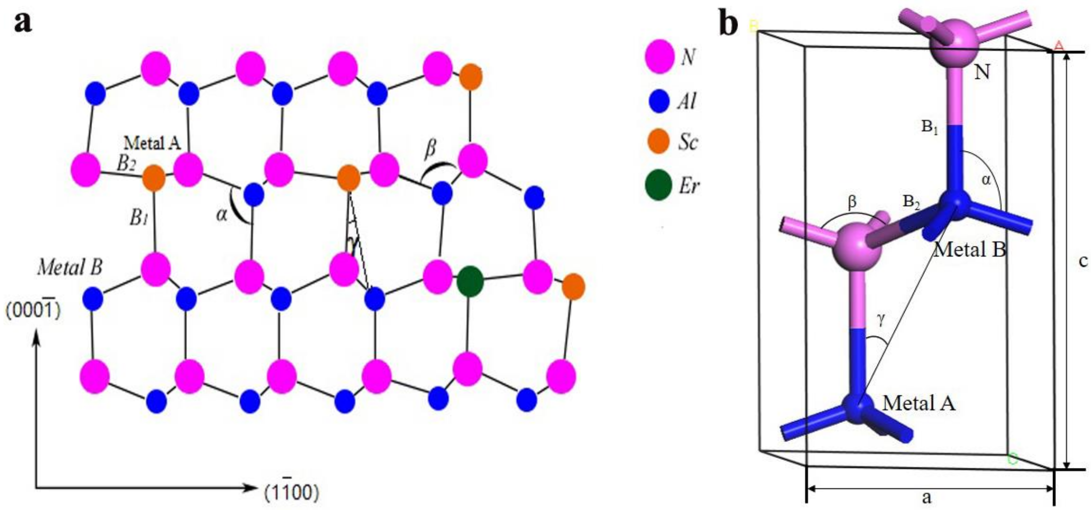

Figure.3 (a) *c*-axis growth pattern of the Er and Sc co-doped films (b) the unit cell

The Metal A and Metal B represent different chemical environment of Al atom relative to the same N atom, respectively. The bond angle ***γ*** is the angle between the metal-metal bond and the nearest N-metal bond. The *c/a*-axis ratio, which is proportional to *α* and inversely proportional to the bond angle B_2/B_1 can be calculated as

$$c/a = \frac{2}{\sqrt{3}} \cdot \sqrt{\frac{1}{sin^2\gamma} - 1} \qquad (1)$$

The unit cell parameters in Table 1 are obtained by fitting GIXRD curves. From the data in Table 1, it can be obtained that the incorporation of Sc and Er atoms into the AlN film would stretch the bond lengths of B_1, B_2 as well as the lattice constants. As shown in the Figure.4, the *c/a* value increases with Er/Sc ratio in the co-doped films but decreases in either Er or Sc single-doped films. The Figure.4 also shows that the *c/a* proportional to *α* and inversely proportional to B_2/B_1 in co-doped films, which accords with the result obtained from the AlN unit cell.

Table 1 Cell parameter fitting data of $Er_xSc_yAl_{1-x-y}N$ films

Sample	a (Å)	b (Å)	c (Å)	B1 (Å)	B2 (Å)	α (°)	β (°)	γ (°)	B2/B1	c/a	Volume (Å^3)	χ^2
AlN	3.142	3.142	5.002	1.911	1.908	108.02	110.882	35.96	0.999	1.592	42.76	1.62
$Sc_{0.11}Al_{0.89}N$	3.176	3.176	5.017	1.917	1.927	107.89	111.000	36.17	1.005	1.579	43.83	1.61
$Er_{0.03}Sc_{0.08}Al_{0.89}N$	3.182	3.182	5.04	1.925	1.931	107.94	110.960	35.97	0.997	1.583	44.19	1.34
$Er_{0.07}Sc_{0.04}Al_{0.89}N$	3.218	3.218	5.107	1.951	1.953	107.97	110.928	36.04	1.001	1.587	45.77	1.20
$Er_{0.09}Sc_{0.02}Al_{0.89}N$	3.165	3.165	5.154	1.969	1.926	108.41	110.513	35.39	0.978	1.628	44.72	1.23
$Er_{0.11}Al_{0.89}N$	3.214	3.204	5.107	1.951	1.946	108.04	110.861	35.94	0.997	1.589	45.42	1.26

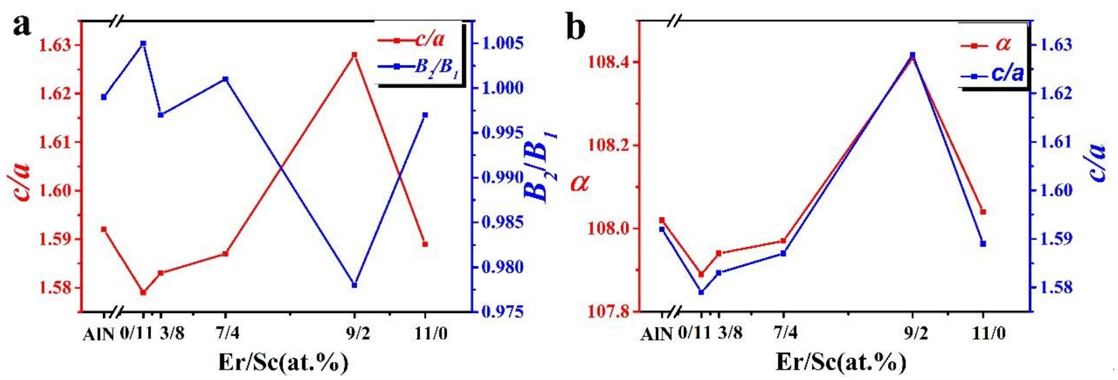

Figure.4 (a) The *c/a* and B_2/B_1 (b) the *α* and *c/a* of Er and Sc co-doped films

As Sc-doped AlN films, the ScN has a hexagonal structure which is similar to *h*-BN [17, 18], Sc atoms and Al atoms tend to form a six-coordinate structure, resulting in a decrease of bond angle *α*, as well as the decrease of *c/a*. According to Pauling's principle [19], the ionic composition of Er-N bond is 55.5%, which is larger than 50.6% of Sc-N. The bond energy of Er-N is lower than that of Sc-N, and the bond length of

Er-N is larger than that of Sc-N. In the co-doped AlN films, some Sc atoms in the Metal A position will be replaced by Er atoms, which resulting the ratio of B_1 bonds increases much faster than that of B_2 bond. Therefore, the *c/a* ratios of the co-doped films are much higher than that of Sc doped film. Besides, the radius of Er^{3+} is larger than those of Al^{3+} and Sc^{3+}, the extremely large value of *c/a* for the film of $Er_{0.09}Sc_{0.02}Al_{0.89}N$ can be attributed to the increased amount of Er, which causes the increase of bond angle α, and the increased expansion in the *c*-axis. Er has priority in replacement of Metal B position in Al sites, so for the AlN film single-doped with Er, the expansion rate of B_2 bond is faster than that of B_1 bond, thus the *c/a* value decreases compared with Er and Sc co-doped AlN film.

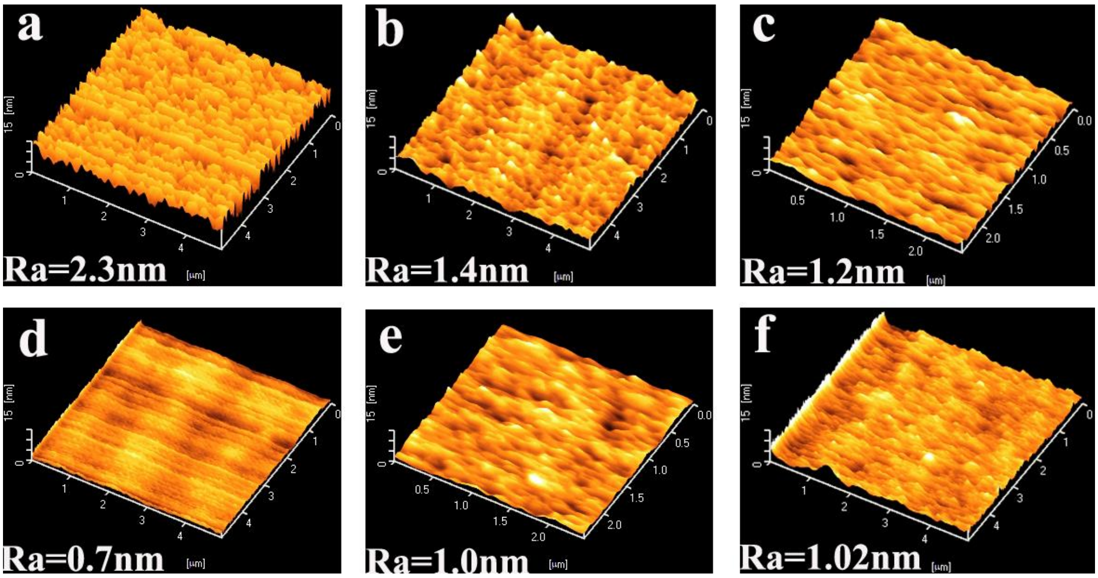

Figure.5 Surface topography of AlN films with different Er/Sc ratios of (a) pure AlN (b) 0/11 (c) 3/8 (d) 7/4 (e) 9/2 (f) 11/0

Figures 5(a) ~ 4(f) show that the surface roughness of doped AlN films is between 0.7 to 2.3 nm, which are able to meet the standard of SAW device's fabrication. Figure 6 shows the measured transmission signals (S_{21}) of the SAW devices with λ of 16 μm.

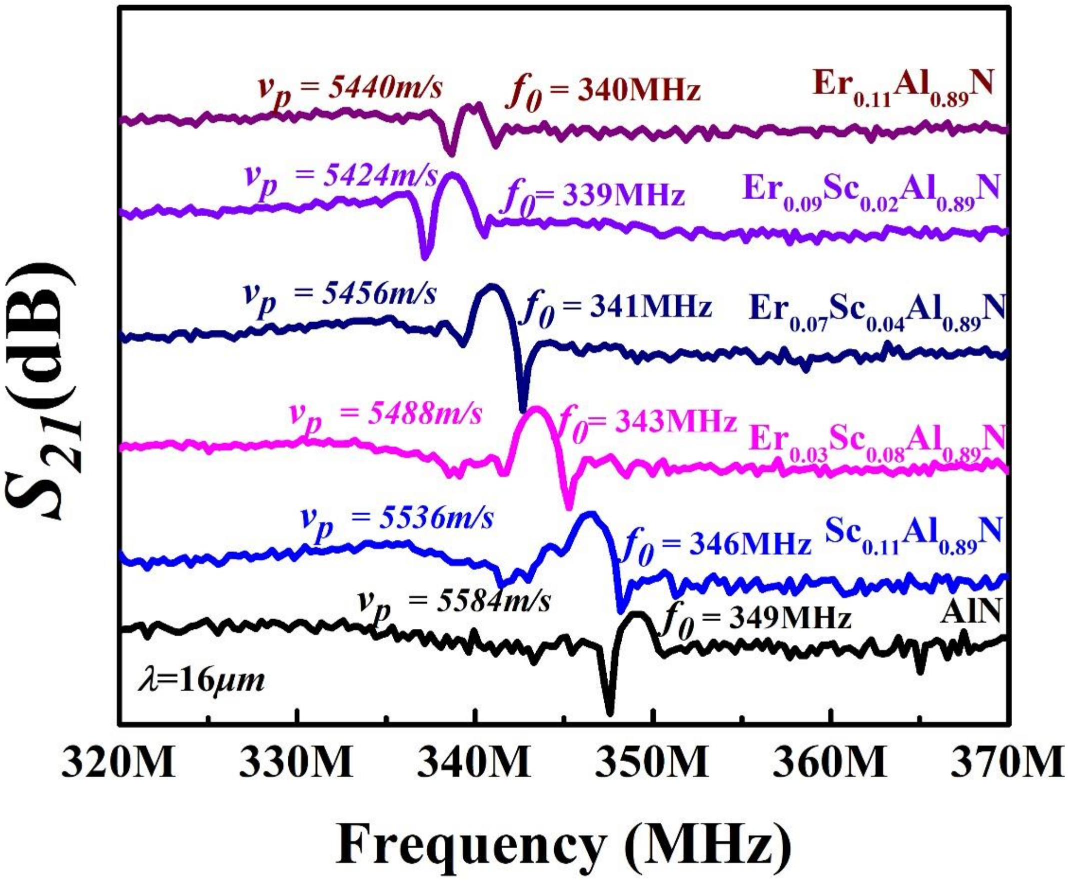

Figure.6 S_{21} curve of $Er_xSc_yAl_{1-x-y}N$ film-based SAW devices

As shown in Figure 6, all the devices show the resonance responses (ranging from 335 MHz to 350 MHz). The center frequency f_0 of SAW filters decrease from 349 MHz to 339 MHz, with the relative content of Er increased from 0 to 0.09. According to $v_p = \lambda f_0$, the calculated phase velocity (v_p) values of these SAW filters decrease gradually when the content of Er increases from 0 to 0.09.-The reduction of acoustic velocity is related to the elastic softening or the increase of the density, or both. [20, 21] The density of co-doped AlN film is affected by the doped atom mass and defects of film, which increases with the doping contents of both Er and Sc. The *c/a* ratio of co-doped AlN film increases with the amount of Er, indicating that the crystal structure is not softened. That is, the reduction of acoustic velocity from $Sc_{0.11}Al_{0.89}N$ film to $Er_{0.09}Sc_{0.02}Al_{0.89}N$ film is mainly due to the increase of value of □$_{f□□}$. Since the crystal structure becomes softened and stiffness coefficient C_f decreases from pure AlN to $Sc_{0.11}Al_{0.89}N$ film, the reduction of value of v_p can be attributed to the combined effects of decreased C_f and increased density of the film.

Electromechanical coupling coefficient k^2_{eff} is corresponding to energy transduction efficiency between the electrical and mechanical domains, which is mainly dependent upon the piezoelectric properties of the film. It can be deduced that the increase of k^2_{eff} is related to the reduction of *c/a* and the crystal structure softening for doped AlN films. [10,11] Therefore, the values of k^2_{eff} decrease with the increase of *c/a* in this research.

According to the equivalent circuit of a SAW transducer, the electromechanical coupling coefficient k^2_{eff} can be obtained by formula (2) [22]:

$$k_{eff}^2 = \pi G_m(f_0)/4NB_s(f_0) \quad (2)$$

where N is the finger pairs, G_m (f_0) and B_s (f_0) are the motional conductance and static susceptance of the input port at resonant frequency, respectively. The obtained results of k^2_{eff} are plotted in Figure 7. The k^2_{eff} value is inversely proportional to the *c/a* value, which is consistent with theoretical analysis discussed above. The $Sc_{0.11}Al_{0.89}N$ film has the largest k^2_{eff} value of 2.79%, and the $Er_{0.09}Sc_{0.02}Al_{0.89}N$ obtains the smallest k^2_{eff} value of 1.44%, which are related to their *c/a* values (which are the minimum and maximum values). The k^2_{eff} of pure AlN was calculated to be 2.04%, which agrees with the value

(2%) reported in literature [7]. The k^2_{eff} of the $Er_{0.11}Al_{0.89}N$ SAW device is 2.14%, which is slightly higher than that of pure AlN, but much higher than that of $Er_{0.09}Sc_{0.02}Al_{0.89}N$ SAW device.

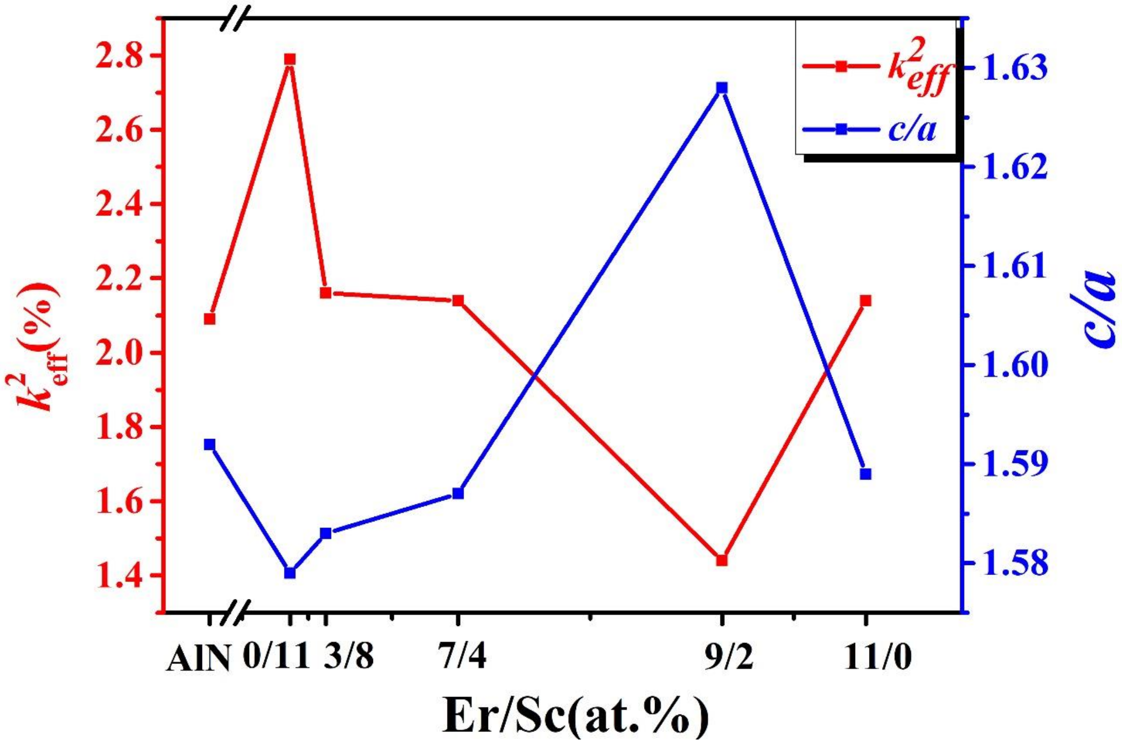

Figure.7 the k^2_{eff} and *c/a* of the $Er_xSc_yAl_{1-x-y}N$ film

Thus, the piezoelectric property of AlN films doped with Er and Sc is worse than that of either Er or Sc single doped AlN films, which is related to the softening degree of crystal structure.

4. Conclusion

All the deposited $Er_xSc_yAl_{1-x-y}N$ films exhibit a strong texture of *c*-axis orientation and a pure wurtzite AlN structure after doped with different elements. Compared with that of the pure AlN film, the *c/a*-axis ratio decreases after the Sc doping, while the value of *c/a* increases with the amount of Er increases from 0% up to 0.09%, but then decreases in $Er_{0.11}Al_{0.89}N$ film. These results show that the piezoelectric response of the films decreases with the increase of Er/Sc ratio in Sc/Er co-doped films, whereas the reverse data is obtained for the single-doping with either Er or Sc. For the SAW resonator based on $Er_xSc_yAl_{1-x-y}N$ film, results show that the k^2_{eff} of the SAW resonator is inversely proportional to the *c/a*-axis ratio of the doped AlN film, and the piezoelectric responses of Sc and Er co-doped films decrease compared with those of doping with either Er or Sc.

ACKNOWLEDGMENT

This work was supported by the National Natural Science Foundation of China (NFSC No. 51605485). Engineering Physics and Science Research Council of UK (EPSRC EP/P018998/1) and Newton Mobility Grant (IE161019) through Royal Society and NFSC.

REFERENCES

[1] Butcher K S A, Tansley T L. Ultrahigh resistivity aluminum nitride grown on mercury cadmium telluride [J]. Journal of Applied Physics, 2001, 90(12):6217-6221.

[2] Mortet V, Vasin A, Jouan P Y, et al. Aluminium nitride films deposition by reactive triode sputtering for surface acoustic wave device applications [J]. Surface & Coatings Technology, 2003, 176(1):88-92.

[3] P. Limsuwan, n. Udomkan, s. Meejoo, et al. Surface morphology of submicron crystals in aluminum nitride films grown by dc magnetron sputtering [J]. International Journal of Modern Physics B, 2005, 19(12):2073-2083.

[4] Lei W, Shuming C, Jinying Z, et al. High performance 33.7 GHz surface acoustic wave nanotransducers based on AlScN/diamond/Si layered structures [J]. Applied Physics Letters 113(9):093503.

[5] Mehadi H Z, Koel Ants. Design and Optimization of AlN based RF MEMS Switches [J]. IOP Conference Series: Materials Science and Engineering, 2018, 362:012002-.

[6] Akiyama M, Kamohara T, Kano K, et al. Enhancement of piezoelectric response in scandium aluminum nitride alloy thin films prepared by dual reactive cosputtering [J]. Advanced Materials, 2009, 21(5):593.

[7] Zou J, Lin C M, Lam C S, et al. Transducer design for AlN Lamb wave resonators [J]. Journal of Applied Physics, 2017, 121(15):154502.

[8] Iwazaki Y, Yokoyama T, Nishihara T, et al.Highly enhanced piezoelectric property of co-doped AlN [J]. Applied Physics Express, 2015, 8(6):061501.

[9] Wingqvist G, Tasnadi F, Zukauskaite A, et al. Increased electromechanical coupling in w-ScxAl1-xN [J]. Applied Physics Letters, 2010, 97(11):593.

[10] Uehara M , Shigemoto H , Fujio Y , et al. Giant increase in piezoelectric coefficient of AlN by Mg-Nb simultaneous addition and multiple chemical states of Nb[J]. Applied Physics Letters, 2017, 111(11):112901.

[11] Zhang S , Holec D , Fu W Y , et al. Tunable optoelectronic and ferroelectric properties in Sc-based, III-nitrides[J]. Journal of Applied Physics, 2013, 114(13):77-R.

[12] Ferenc Tasnádi, Björn Alling, Carina Höglund, et al. Origin of the anomalous piezoelectric response in wurtzite ScxAl1-xN alloys [J]. Physical Review Letters, 2010, 104(13):137601.

[13] Zywitzki O, Modes T, Barth S, et al. Effect of scandium content on structure and piezoelectric properties of AlScN films deposited by reactive pulse magnetron sputtering [J]. Surface and Coatings Technology, 2016:S0257897216312129.

[14] Narang V, Korakakis D, Seehra M S. Electronic state of Er in sputtered AlN:Er films determined by magnetic measurements[J]. Journal of Applied Physics, 2014, 116(21):213911.

[15] Narang V, Korakakis D. Effects of Erbium alloying on the structural and piezoelectric properties of Aluminum Nitride thin films annealed under extreme thermal conditions [J]. MRS Proceedings, 2013, 1519:mrsf12-1519-mm03-28.

[16] Mayrhofer P M, Eisenmenger-Sittner C, Stoeger-Pollach M, et al. The impact of argon admixture on the c-axis oriented growth of direct current magnetron sputtered ScxAl1−xN thin films [J]. Journal of Applied Physics 115, 193505 (2014).

[17] Holec D, Franz R, Mayrhofer P H, et al. Structure and stability of phases within the NbN–AlN system[J]. Journal of Physics D Applied Physics, 2010, 43(14):145403

[18] Takeuchi N. First-principles calculations of the ground-state properties and stability of ScN [J].Physical Review B, 2002, 65(4):321-325

[19] Bratsch S G. Electronegativity equalization with Pauling units [J]. Journal of chemical education, 1984, 61(7):588-589.

[20] Caro M A, Zhang S , Riekkinen T , et al. Piezoelectric coefficients and spontaneous polarization of ScAlN[J]. Journal of Physics: Condensed Matter, 2015, 27(24):245901.

[21] Deger C, Born E, Angerer H, et al. Sound velocity of AlxGa1-xN thin films obtained by surface acoustic-wave measurements [J]. Applied Physics Letters, 1998, 72(19):2400-0.

[22] Jin H , Zhou J , He X , et al. Flexible surface acoustic wave resonators built on disposable plastic film for electronics and lab-on-a-chip applications[J]. Scientific Reports, 2013, 3(7):2140.